USGS
science for a changing world

Application of Decline Curve Analysis To Estimate Recovery Factors for Carbon Dioxide Enhanced Oil Recovery

By Hossein Jahediesfanjani

Chapter C of
Three Approaches for Estimating Recovery Factors in Carbon Dioxide Enhanced Oil Recovery
Mahendra K. Verma, Editor

Scientific Investigations Report 2017–5062–C

U.S. Department of the Interior
U.S. Geological Survey

U.S. Department of the Interior
RYAN K. ZINKE, Secretary

U.S. Geological Survey
William H. Werkheiser, Acting Director

U.S. Geological Survey, Reston, Virginia: 2017

Suggested citation:
Jahediesfanjani, Hossein, 2017, Application of decline curve analysis to estimate recovery factors for carbon dioxide enhanced oil recovery, chap. C *of* Verma, M.K., ed., Three approaches for estimating recovery factors in carbon dioxide enhanced oil recovery: U.S. Geological Survey Scientific Investigations Report 2017–5062, p. C1–C20, https://doi.org/10.3133/sir20175062C.

ISSN 2328-0328 (online)

Contents

Figures

Tables

Chapter C. Application of Decline Curve Analysis To Estimate Recovery Factors for Carbon Dioxide Enhanced Oil Recovery

By Hossein Jahediesfanjani[1]

Background

In the decline curve analysis (DCA) method of estimating recoverable hydrocarbon volumes, the analyst uses historical production data from a well, lease, group of wells (or pattern), or reservoir and plots production rates against time or cumulative production for the analysis. The DCA of an individual well is founded on the same basis as the fluid-flow principles that are used for pressure-transient analysis of a single well in a reservoir domain (Fetkovich, 1987; Fetkovich and others, 1987) and therefore can provide scientifically reasonable and accurate results. However, when used for a group of wells, a lease, or a reservoir, the DCA becomes more of an empirical method. Plots from the DCA reflect the reservoir response to the oil withdrawal (or production) under the prevailing operating and reservoir conditions, and they continue to be good tools for estimating recoverable hydrocarbon volumes and future production rates. For predicting the total recoverable hydrocarbon volume, the DCA results can help the analyst to evaluate the reservoir performance under any of the three phases of reservoir productive life—primary, secondary (waterflood), or tertiary (enhanced oil recovery) phases—so long as the historical production data are sufficient to establish decline trends at the end of the three phases.

Basis for Decline Curve Analysis

The DCA method is used to predict the future oil production rate of an oil-producing well or reservoir. Theoretically, according to this method, the oil production rate for a given entity will first reach its maximum output and then decline according to the following generalized relationship (Fetkovich, 1987):

$$\frac{q}{q_i} = (1 + bD_i t)^{-\frac{1}{b}} \tag{C1}$$

where

q is the time-dependent oil production rate, in barrels per day (bbl/day);

q_i is the initial oil production rate, in barrels per day;

D_i is the initial decline rate per year;

b represents the degree of curvature of the shape of the decline trend, which is dimensionless; and

t is the oil production time, in years.

Theoretically, the parameters, such as q_i, D_i, and b, have defined meanings only if equation C1 is applied for a single well that produces from a single reservoir under appropriate fluid-flow conditions. However, if equation C1 is applied to larger entities such as a number of wells, a reservoir, or a field, these parameters are only empirical and are obtained by a curve-fitting process. Practically, this equation represents three different types of declines depending on the value of b; namely, an exponential decline for $b = 0$, a hyperbolic decline for $b > 0$ and $b < 1$, and a harmonic decline for $b = 1$. On the basis of the explanations above and for the sake of simplicity, in many of the industrial applications of evaluating reservoir oil production decline, the value of b is often assumed to be zero, and, hence, equation C1 takes the form:

$$q = q_i \exp(-D_i t) \tag{C2}$$

[1]Lynxnet LLC, under contract to the U.S. Geological Survey.

Equation C2 is rewritten in terms of cumulative oil production in the following form:

$$Q = \frac{(q_i - q)}{D_i} \tag{C3}$$

where

Q is the cumulative oil production, in barrels.

These two equations, C2 and C3, were used for the analysis of oil production decline in this current study to determine the values of constants "D_i" and "q_i" in the above equations. For this purpose, these equations can be written as:

$$\ln(q) = \ln(q_i) - D_i t \tag{C4}$$

$$q = q_i - D_i Q \tag{C5}$$

On the basis of equation C4, plotting the oil production rate (q) versus production time (t) on a semi-log graph will result in a straight line having an intercept equal to $\ln(q_i)$ and a slope equal to D_i. Alternatively, on the basis of equation C5, plotting the oil production rate (q) versus cumulative oil production (Q) will result in a straight line having an intercept and slope equal to q_i and D_i, respectively. After values are determined for D_i and q_i, equations C4 and C5 are used to predict the future oil production rate and the cumulative amount of recoverable oil, respectively. The current assessment methodology is designed to assess only the technically recoverable hydrocarbon for the carbon dioxide enhanced oil recovery (CO_2-EOR) application, implying no economic limit. If an economic evaluation is required in the future, first an appropriate economic hydrocarbon production rate (q_{ec}) in reservoir barrels per day (bbl/day) needs to be defined below which hydrocarbon production from a given reservoir is considered to be uneconomic. The magnitude of the introduced value of q_{ec} depends on each project configuration and specifications and external factors such as hydrocarbon prices that vary from one project to another. After the value of q_{ec} is chosen, the field's productive life (t_{ec}) and total economically recoverable hydrocarbon volume (Q_{ec}) can be calculated by applying the following equations:

$$t_{ec} = -\frac{1}{D_i}\ln\left(\frac{q_{ec}}{q_i}\right) \tag{C6}$$

$$Q_{ec} = -\frac{1}{D_i}(q_i - q_{ec}) \tag{C7}$$

For a technically recoverable hydrocarbon volume, designated as Q_{max}, the recovery factor (RF) under current production conditions is estimated from the following:

$$RF = \frac{Q_{max}}{OOIP} \times 100 \tag{C8}$$

where

Q_{max} is the maximum cumulative oil production, in barrels (bbl);

$OOIP$ is the original oil in place, in stock tank barrels (STB); and

RF is the recovery factor, expressed as a percentage.

If an incremental recovery factor is required for any phase (that is, primary, secondary, or tertiary), it is determined as the total calculated RF at phase i minus the total calculated RF at the previous phase ($i - 1$):

$$RF_{Incremental} = RF_i - RF_{i-1} \tag{C9}$$

where

i is 1 for primary, 2 for secondary, and 3 for tertiary production.

For example, if the reservoir is currently under CO_2-EOR, which was initiated after a waterflood, the calculated RF at the current stage represents the total recovery, including all three stages of primary, waterflood, and CO_2-EOR. Therefore, on the basis of equation C9, the additional recovery factor due to CO_2-EOR is obtained by subtracting the calculated RF values of the waterflood from the RF value calculated for the CO_2-EOR.

Case Study

The Oil and Gas Journal's 2012 survey of EOR projects (Koottungal, 2012; Kuuskraa, 2012) indicated that about 123 CO_2-EOR projects were active within the United States in 2012. Twenty-four fields (28 reservoirs) of these projects were initially selected for DCA. However, after the initial investigation, almost half of these projects were excluded from the DCA because they either did not develop long enough CO_2-EOR decline periods appropriate for the DCA or were not in their decline phases yet. Data for the DCA were obtained from the comprehensive resource database (CRD), which was described by Carolus and others (in press); the CRD was developed from two proprietary databases by Nehring Associates Inc. (2012) and IHS Inc. (2012) and provided adequate injection and production data for only 12 fields containing 15 reservoirs. Therefore, the DCA was successfully applied

only on these fields that have established a good CO_2-EOR decline trend. The results of DCA on 15 reservoirs from these 12 fields are summarized in table C1 (tables follow the "References Cited"). The DCA for the Sable oil field in the west Texas section of the Permian Basin Province is presented here to show the procedure, and the details of the DCA for all the 15 reservoirs are provided in appendix C1. It is important to note that the Sable oil field was under a CO_2-EOR operation from 1984 to 2001 and hence was not an active CO_2-EOR project in 2012. However, because it makes a great example of the application of DCA, this field is being analyzed and presented herein.

In order to present the DCA procedure and demonstrate its applicability in modeling both waterflood and CO_2-EOR decline periods for the Sable oil field, two figures were generated and are discussed. Figure C1 shows the semi-log plot of oil production rate versus production time for the Sable oil field. This graph shows that the oil production decline during waterflood that began in 1976 continued until 1984, when the CO_2-EOR project was initiated. Because of CO_2-EOR, the field production remained stable until 1993, when the production decline started again.

Figure C2 shows the oil production rate versus the cumulative oil production for the Sable oil field. As shown in the figure, the technically recoverable oil volume has increased from 9.85 million barrels (MMbbl) for the waterflood phase to 13.1 MMbbl for the CO_2-EOR phase.

The oil production data for DCA are from IHS Inc. (2012), and the calculated *OOIP* values are from the CRD (Carolus and others, in press), which is based on data from the Nehring Associates Inc. database (2012) and IHS Inc. (2012). Because the *OOIP* values from the CRD are proprietary, the *OOIP* values of reservoirs are reported qualitatively in table C2 and appendix C1 as small, medium, and large: a small *OOIP* is less than or equal to 100 MMbbl, a medium *OOIP* is between 100 and 1,000 MMbbl, and a large *OOIP* is larger than or equal to 1,000 MMbbl. The *OOIP* of the San Andres Limestone of the Sable oil field was estimated volumetrically to be less than 100 MMbbl, thus classifying the reservoir in the Sable field as a small reservoir. By applying equation C8, the calculated recovery factors are 27.2 and 36.2 percent for waterflood and CO_2-EOR, respectively (table C2). On the basis of equation C9, the additional recovery-factor value due to CO_2-EOR is 9.0 percent. A similar process has been repeated for the selected 14 reservoirs located in Colorado, Wyoming, and the Permian Basin of Texas and New Mexico that were under CO_2-EOR in 2012.

The additional recoverable oil volumes for CO_2-EOR in 15 selected reservoirs were estimated by using DCA. Recovery factors were calculated by dividing the recoverable oil volumes at the end of the waterflood and at the end of CO_2-EOR by the *OOIP* of the individual reservoirs.

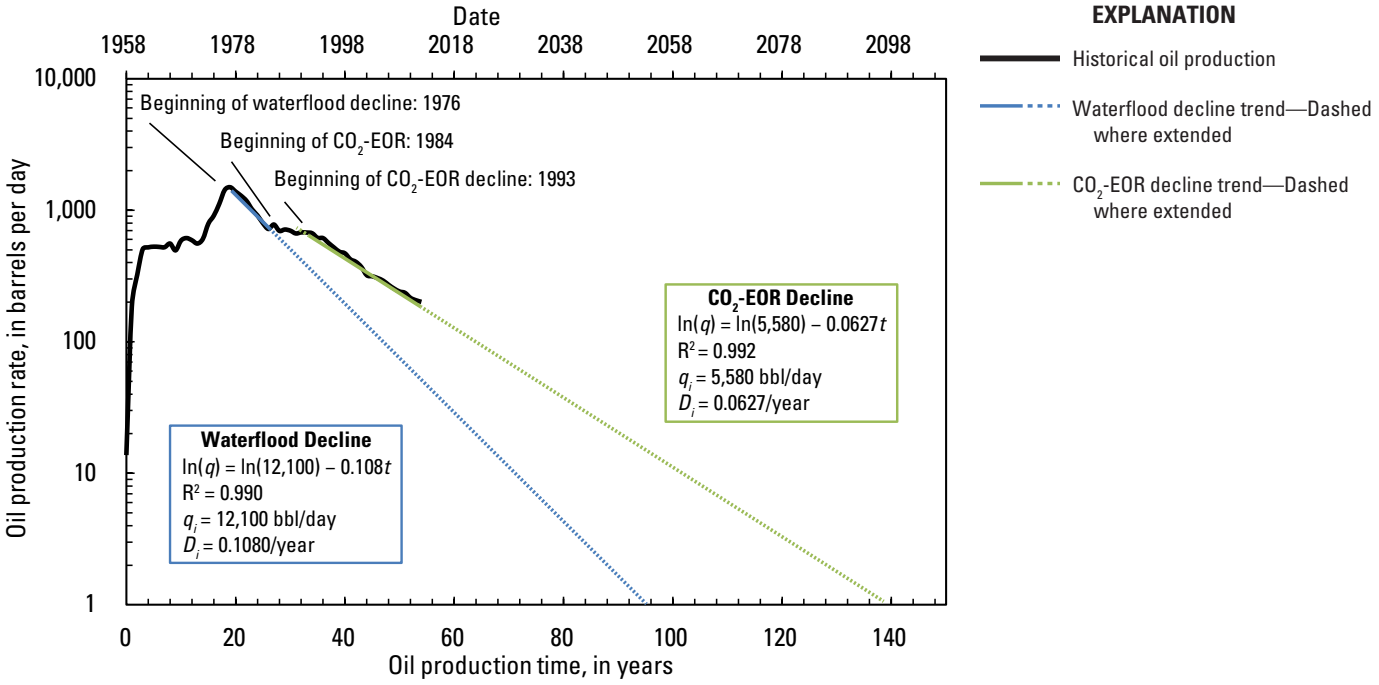

Figure C1. Semi-log plot of the oil production rate versus the oil production time for the San Andres Limestone in the Sable oil field in the west Texas section of the Permian Basin Province, showing the decline trends for both the waterflood and the carbon dioxide enhanced oil recovery (CO_2-EOR) phases. Data are from IHS Inc. (2012). Terms used in the decline equations on the graph: D_i = initial decline rate per year; q = oil production rate, in barrels per day (bbl/day); q_i = initial oil production rate, in barrels per day (bbl/day); R^2 = coefficient of determination; t = oil production time, in years.

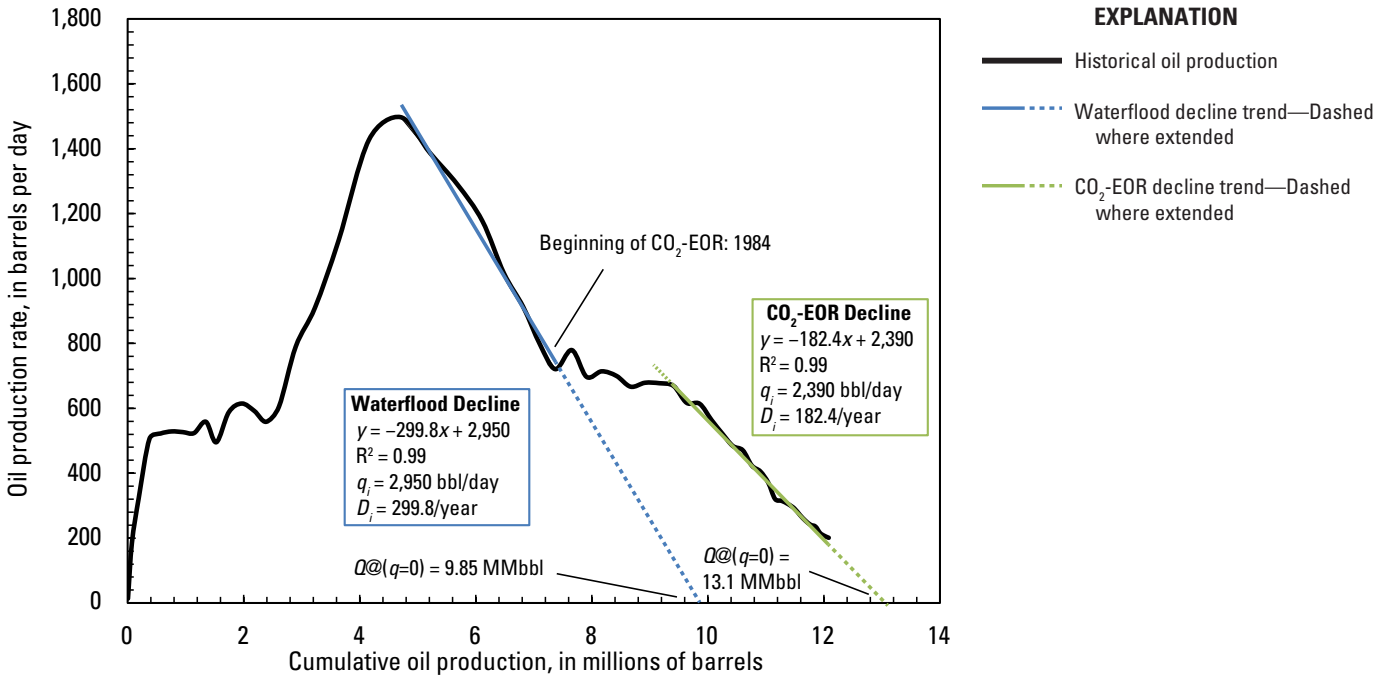

Figure C2. Graph of the oil production rate versus the cumulative oil production for the San Andres Limestone in the Sable oil field, Texas, showing the decline trends for both the waterflood and the carbon dioxide enhanced oil recovery (CO_2-EOR) phases. Data are from IHS Inc. (2012). Terms used in the decline equations on the graph: D_i = initial decline rate per year; q = oil production rate, in barrels per day (bbl/day); q_i = initial oil production rate, in barrels per day (bbl/day); Q = cumulative oil production, in millions of barrels (MMbbl); R^2 = coefficient of determination; x = cumulative oil production in the trendline equation, in millions of barrels; y = oil production rate in the trendline equation, in barrels per day.

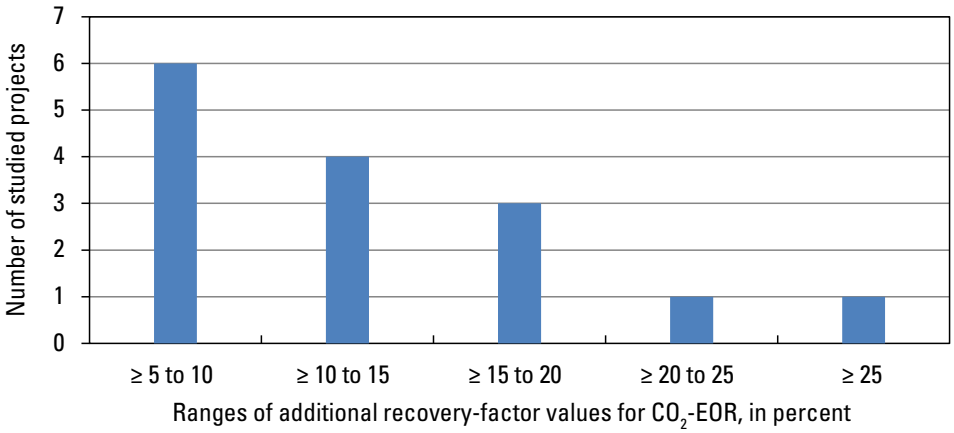

Figure C3. Bar graph showing the number of studied reservoirs having values of additional oil recovery factors due to carbon dioxide enhanced oil recovery (CO_2-EOR) in five different ranges. Recovery-factor values estimated by decline curve analysis are from table C2.

Discussion

Generally speaking, the DCA is utilized in this study as a method that enables calculating both current and projected values of reservoir oil recovery-factor values at the end of a waterflood period and a subsequent CO_2-EOR period. Table C1 summarizes the best match values of the initial oil production rate (q_i) and the initial decline rate for oil production (D_i) and the corresponding values of the coefficient of determination (R^2) values in the DCA equation for both waterflood and CO_2-EOR decline periods of the studied reservoirs. As explained above, the q_i and D_i values are empirical matching parameters and do not carry any physical meanings. For comparison purposes, it can be observed from this table that the overall average values of q_i and D_i are 72,500 bbl/day and 360.7/year for the waterflood period and 125,400 bbls/day and 190.5/year for the CO_2-EOR period, respectively. It is important to note that the overall average values of R^2 are 0.951 and 0.952 for the waterflood and CO_2-EOR periods, respectively, indicating a good to excellent match for the waterflood and CO_2-EOR periods. This observation highlights an important point that the basic DCA method as it has been routinely applied to model waterflood decline in performance analysis can also be utilized to model the CO_2-EOR decline period with similar accuracy.

The calculated recovery factors for the technically recoverable oil volumes for the waterflood and CO_2-EOR phases and the additional oil recovery for the CO_2-EOR phase for all 15 studied reservoirs are reported in table C2. The results of this table indicate that the incremental oil recovery factor by CO_2-EOR ranges from 6.6 percent for the Weber Sandstone in the Rangely field to 25.7 percent for the San Andres Limestone (dolomite) in the Wasson field, whereas the average overall calculated recovery factor for the studied reservoirs is 13.2 percent. The ranges of the additional recovery factor due to CO_2-EOR from DCA along with the values from the review of literature on CO_2-EOR in chapter D are utilized to substantiate the estimated values from the reservoir modeling as described in chapter B.

Data from table C2 reveal that the average additional recovery factor with CO_2-EOR from the seven dolomite reservoirs producing from the San Andres Limestone is around 13.5 percent, whereas the other five carbonate reservoirs have an average additional recovery of 14.3 percent. The average additional recovery factor for the 3 clastic (sandstone) reservoirs is 10.9 percent, which is lower than the 13.8 percent for the 12 carbonate reservoirs. However, the data are limited in terms of samples and, therefore, it is hard to make any conclusive observations. In figure C3, the reservoirs that were evaluated for DCA are grouped according to their *RF* values for CO_2-EOR, and the graph shows that most of them are in the lower range (13 out of 15 are less than 20 percent)—6 are in the range of ≥5 to 10 percent, 4 are in the range of ≥10 to 15 percent, and 3 are in the range of ≥15 to 20 percent.

From the lithology point of view, the majority of the studied reservoirs (12 out of 15) are carbonates and only 3 are sandstone reservoirs. This small sample size of sandstone reservoirs makes the comparison of the CO_2-EOR performance in these two lithological classes practically impossible.

References Cited

Carolus, Marshall, Biglarbigi, Khosrow, Warwick, P.D., Attanasi, E.D., Freeman, P.A., and Lohr, C.D., in press, Overview of a comprehensive resource database for the assessment of recoverable hydrocarbons produced by carbon dioxide enhanced oil recovery: U.S. Geological Survey Techniques and Methods, book 7, chap. C16.

Fetkovich, M.J., 1980, Decline curve analysis using type curves: Journal of Petroleum Technology, v. 32, no. 6 (June 1980), p. 1065–1077, paper SPE–4629–PA.

Fetkovich, M.J., Vienot, M.E., Bradley, M.D., and Kiesow, U.G., 1987, Decline curve analysis using type curves—Case histories: SPE (Society of Petroleum Engineers) Formation Evaluation, v. 2, no. 4 (December 1987), p. 637–656, paper SPE–13169–PA.

Holm, L.W., and Josendal, V.A., 1974, Mechanisms of oil displacement by carbon dioxide: Journal of Petroleum Technology, v. 26, no. 12 (December 1974), p. 1427–1438, paper SPE–4736–PA.

IHS Inc., 2012, PIDM [Petroleum Information Data Model] relational U.S. well data [data current as of December 23, 2011]: Englewood, Colo., IHS Inc.

Koottungal, Leena, ed., 2012, 2012 worldwide EOR survey: Oil and Gas Journal, v. 110, no. 4 (April 2, 2012), p. 1–4, accessed in 2014 at http://www.ogj.com/articles/print/vol-110/issue-4/general-interest/special-report-eor-heavy-oil-survey/2012-worldwide-eor-survey.html.

Kuuskraa, Vello, 2012, QC updates carbon dioxide projects in OGJ's enhanced oil recovery survey: Oil and Gas Journal, v. 110, no. 7 (July 2, 2012), p. 1–4, accessed [in 2014] at http://www.ogj.com/articles/print/vol-110/issue-07/drilling-production/qc-updates-carbon-dioxide-projects.html.

Nehring Associates Inc., 2012, Significant oil and gas fields of the United States database [data current as of December 2012]: Colorado Springs, Colo., Nehring Associates Inc.

Table C1. Best match values of the initial oil production rate, the initial decline rate for oil production, and the corresponding coefficient of determination (R^2) values for both waterflood and carbon dioxide enhanced oil recovery (CO_2-EOR) decline periods of the studied reservoirs.

[The selection of the 15 studied reservoirs and the sources of data are described in chapter C of this report. Fourteen of the reservoirs had active CO_2-EOR projects in 2012. The reservoir in the Sable oil field did not have an active CO_2-EOR project in 2012, but it is included because it is a good example. The values in this table were determined by decline curve analysis. Each reservoir is described as a case study in appendix C1. State abbreviations: CO, Colorado; NM, New Mexico; TX, Texas; WY, Wyoming. Variables: D_i, initial decline rate per year in oil production; q_i, initial oil production rate, in barrels per day (bbl/day)]

Case study number in appendix C1	Oil field	State	Stratigraphic unit containing the reservoir	Waterflood			CO_2-EOR		
				q_i (bbl/day)	D_i (/year)	R^2	q_i (bbl/day)	D_i (/year)	R^2
1	Sable*	TX	San Andres Limestone	2,950	299.8	0.99	2,390	182.4	0.99
2	Rangely	CO	Weber Sandstone	89,500	215.9	0.98	88,000	169.9	0.92
3	Lost Soldier	WY	Tensleep Formation	18,000	427.8	0.95	23,000	314.3	0.96
4	Lost Soldier	WY	Madison Formation	6,900	497.9	0.98	8,500	329.9	0.96
5	Wasson	TX	San Andres Limestone	421,000	300.9	0.98	120,000	43.1	0.95
6	Wasson	TX	Clear Fork Group	26,000	279.3	0.99	20,000	65.0	0.93
7	Dollarhide	TX	Thirtyone Formation	23,000	405.9	0.89	11,000	87.6	0.85
8	Dollarhide	TX	Clear Fork Group	7,500	426.8	0.95	9,000	213.3	0.97
9	Salt Creek	TX	“Canyon-age reservoir”	49,000	154.3	0.94	116,000	295.1	0.96
10	Seminole	TX	San Andres Limestone	106,000	232.3	0.87	97,000	129.4	0.96
11	Twofreds	TX	Ramsey Member	6,000	1,042.5	0.91	2,400	176.1	0.96
12	Vacuum	NM	San Andres Limestone	61,000	271.6	0.96	44,000	132.7	0.97
13	Cedar Lake	TX	San Andres Limestone	14,000	217.6	0.99	14,500	94.8	0.96
14	North Hobbs	NM	San Andres Limestone	1,200	387.3	0.97	1,900	402.6	0.96
15	Yates	TX	San Andres Limestone	256,000	250.2	0.91	244,000	221.7	0.98
Average				**72,500**	**360.7**	**0.951**	**125,400**	**190.5**	**0.952**

*The Sable oil field was under a CO_2-EOR operation from 1984 to 2001 and hence is not included in the list of CO_2-EOR projects that were active in 2012. Because it makes a great example of the application of decline curve analysis, this field is being analyzed and presented in chapter C and appendix C1 of this report.

Table C2. Additional oil recovery factors estimated by using decline curve analysis for carbon dioxide enhanced oil recovery (CO_2-EOR) projects in 15 selected reservoirs.

[The selection of the 15 studied reservoirs and the sources of data are described in chapter C of this report. Each reservoir is described as a case study in appendix C1. Reservoirs are classified on the basis of the estimated original oil in place (*OOIP*) as small, medium, or large; a small reservoir has less than or equal to100 million barrels (MMbbl) of *OOIP*, a medium reservoir has between 100 and 1,000 MMbbl of *OOIP*, and a large reservoir has more than or equal to 1,000 MMbbl of *OOIP*. State abbreviations: CO, Colorado; NM, New Mexico; TX, Texas; WY, Wyoming. Terms: *RF*, recovery factor; WF, waterflood; %, percent]

Case study number in appendix C1	Oil field	State	Stratigraphic unit containing the reservoir	Lithology	Reservoir size classification	*RF* after WF (%)*	*RF* after CO_2-EOR (%)*	Additional *RF* due to CO_2-EOR (%)
1	Sable**	TX	San Andres Limestone	Dolomite	Small	27.2	36.2	9.0
2	Rangely	CO	Weber Sandstone	Sandstone	Large	26.2	32.8	6.6
3	Lost Soldier	WY	Tensleep Formation	Sandstone	Medium	17.7	30.0	12.3
4	Lost Soldier	WY	Madison Formation	Limestone-dolomite	Medium	8.6	16.2	7.6
5	Wasson	TX	San Andres Limestone	Dolomite	Large	26.2	51.9	25.7
6	Wasson	TX	Clear Fork Group	Dolomite	Large	9.3	30.0	20.7
7	Dollarhide	TX	Thirtyone Formation	Dolomite	Medium	14.8	31.9	17.1
8	Dollarhide	TX	Clear Fork Group	Dolomite	Medium	11.4	27.7	16.3
9	Salt Creek	TX	“Canyon-age reservoir”	Limestone	Large	21.4	31.2	9.8
10	Seminole	TX	San Andres Limestone	Dolomite	Large	18.9	31.0	12.1
11	Twofreds	TX	Ramsey Member	Sandstone	Small	12.4	26.2	13.8
12	Vacuum	NM	San Andres Limestone	Dolomite	Large	19.5	28.9	9.4
13	Cedar Lake	TX	San Andres Limestone	Dolomite	Medium	19.5	27.9	8.4
14	North Hobbs	NM	San Andres Limestone	Dolomite	Small	15.2	33.2	18.0
15	Yates	TX	San Andres Limestone	Dolomite	Large	19.7	31.6	11.9
	Average for clastic (sandstone) reservoirs					**18.8**	**29.7**	**10.9**
	Average for carbonate (mostly dolomite) reservoirs					**17.6**	**31.4**	**13.8**
	Average for all 15 reservoirs					**17.9**	**31.1**	**13.2**

*The obtained recovery factors are based on the projection that both waterflood and CO_2-EOR continue until oil production of zero (q = 0 barrels).

**The Sable oil field was under a CO_2-EOR operation from 1984 to 2001 and hence is not included in the list of CO_2-EOR projects that were active in 2012. Because it makes a great example of the application of decline curve analysis, this field is being analyzed and presented in chapter C and appendix C1 of this report.

Appendix C1. Decline Curve Analysis of Selected Reservoirs

Appendix C1. Decline Curve Analysis of Selected Reservoirs

The 15 reservoirs for case studies of decline curve analysis (DCA) were chosen because adequate geologic, reservoir, and production data were available for them. They all possess specific data on reservoir and fluid properties and vary significantly in terms of (1) size, as is obvious from their reported original oil in place (OOIP), (2) rock types, as they contain both clastic and carbonate reservoirs, (3) geographical locations, being distributed in different basins throughout Texas, New Mexico, Wyoming, and Colorado, and (4) source of carbon dioxide (CO_2), as they use both natural and industrial CO_2. Miscible carbon dioxide enhanced oil recovery (CO_2-EOR) operations were used in 14 reservoirs, and an immiscible operation was used in 1 reservoir (case study 15). Fourteen of the reservoirs had active CO_2-EOR projects in 2012. The reservoir in the Sable oil field (case study 1) did not have an active CO_2-EOR project in 2012, but it is included because it is a good example. The 15 reservoirs all make great examples and case studies in demonstrating the applicability of DCA in predicting the behavior of decline periods for both waterflood and CO_2-EOR phases.

The DCA was applied to the period of declining production of each reservoir separately, and the DCA parameters were obtained by curve fitting. The goodness of the obtained fit is presented by values for the coefficient of determination, R^2, which are reported separately on the graph for each reservoir analyzed (figs. C1–1 to C1–15). The closer the value of R^2 is to 1, the better the quality of the fit. The obtained DCA parameters were utilized to forecast the cumulative oil production when the oil production rates were available over the life of the reservoir for both waterflood and CO_2-EOR phases; for this study, the economic hydrocarbon production rate (q_{ec}) is assumed to be 0 reservoir barrels per day. This process also made it possible to estimate the reservoir's additional oil recovery due to the CO_2-EOR operation that was modeled.

It is important to note that this study does not present the technical and operational details of reservoirs described in the case studies. Nor does it provide a detailed insight into the extent of the CO_2-EOR operation for each investigated project.

Case Study 1. San Andres Limestone, Sable Oil Field

The San Andres Limestone in the Sable oil field in Texas is an oil-bearing dolomite formation that was under CO_2-EOR operation between 1984 and 2001. On the basis of its OOIP, the San Andres Limestone in this field is considered a relatively small oil reservoir. The production decline under waterflood started in 1976 and continued until 1984 when the CO_2-EOR operation was initiated in various sections of the reservoir. As a result of the CO_2-EOR, the field's oil production rate remained stable over the course of 9 years until 1993, when the oil production began to decline again. The details of both waterflood and CO_2-EOR declines and the relevant DCA equations and parameters are presented in figure C1–1.

Case Study 2. Weber Sandstone, Rangely Oil Field

The Weber Sandstone in the Rangely oil field in Colorado is an oil-bearing sandstone formation that was under CO_2-EOR operations in 2012. On the basis of its OOIP, the Weber Sandstone in this field is classified as a large oil reservoir. The waterflood decline of the field started in 1978 and continued until 1986, when the CO_2-EOR operation started in various sections of the reservoir. As a result of the CO_2-EOR, the field's oil production rate increased approximately 10 percent over the course of 5 years until 1991, when the decline in production started again. This reservoir was among the largest clastic reservoirs undergoing CO_2-EOR in 2012. The details of both waterflood and CO_2-EOR declines and the obtained relevant DCA equations and parameters are presented in figure C1–2.

Case Study 3. Tensleep Formation, Lost Soldier Oil Field

The Tensleep Formation in the Lost Soldier oil field in Wyoming is an oil-bearing sandstone formation that was under CO_2-EOR operations in 2012. On the basis of its OOIP, the Tensleep Formation in this field is classified as a medium-sized oil reservoir. The waterflood decline of the field started in 1978 and continued until 1988, when the CO_2-EOR operation started in various sections of the reservoir. As a result of the CO_2-EOR, the field's oil production rate increased approximately 300 percent over the course of 3 years until 1991, when the decline in production started again. The production profile of this reservoir shows two distinct and classical declines for both waterflood and CO_2-EOR periods. The details of both waterflood and CO_2-EOR declines and the obtained relevant DCA equations and parameters are presented in figure C1–3.

Case Study 4. Madison Formation, Lost Soldier Oil Field

The Madison Formation in the Lost Soldier oil field in Wyoming is an oil-bearing carbonate (limestone-dolomite) formation that was under CO_2-EOR operations in 2012. On the basis of its OOIP, the Madison Formation in this field is classified as a medium-sized oil reservoir. The waterflood decline of the field started in 1984 and continued until 1989, when the CO_2-EOR operation started in various sections of the reservoir. As a result of the CO_2-EOR, the field's oil production rate increased approximately 40 percent over the course of 16

years until 2005, when the decline in production started again. The production profile of this reservoir shows two distinct and classical declines for both waterflood and CO_2-EOR periods. The details of both waterflood and CO_2-EOR declines and the obtained relevant DCA equations and parameters are presented in figure C1–4.

Case Study 5. San Andres Limestone, Wasson Oil Field

The San Andres Limestone in the Wasson oil field in the Permian Basin in Texas is an oil-bearing carbonate (dolomite) formation that was under CO_2-EOR operations in 2012. On the basis of its OOIP, the San Andres Limestone in this field is classified as a large oil reservoir. The waterflood decline of the field started in 1975 and continued until 1983, when the CO_2-EOR operation started in various sections of the reservoir. As a result of the CO_2-EOR, the field's oil production decline rate has decreased since. The San Andres Limestone in the Wasson field is one of the largest carbonate reservoirs undergoing CO_2-EOR worldwide. The details of both waterflood and CO_2-EOR declines and the obtained relevant DCA equations and parameters are presented in figure C1–5.

Case Study 6. Clear Fork Group, Wasson Oil Field

The Clear Fork Group in the Wasson oil field in the Permian Basin in Texas is an oil-bearing carbonate (dolomite) formation that was under CO_2-EOR operations in 2012. On the basis of its OOIP, the Clear Fork Group in this field is classified as a large oil reservoir. The waterflood decline of the field started in 1968 and continued until 1984, when the CO_2-EOR operation started in various sections of the reservoir. As a result of the CO_2-EOR, the field's oil production rate increased approximately 93 percent over the course of 13 years until 1997, when it started to decline again. The details of both waterflood and CO_2-EOR declines and the obtained relevant DCA equations and parameters are presented in figure C1–6.

Case Study 7. Thirtyone Formation, Dollarhide Oil Field

The Thirtyone Formation in the Dollarhide oil field in the Permian Basin in Texas is an oil-bearing chert and carbonate (dolomite) formation that was under CO_2-EOR operations in 2012. On the basis of its OOIP, the Thirtyone Formation in this field is classified as a medium-sized oil reservoir. The waterflood decline of the field started in 1965 and continued until 1985, when the CO_2-EOR operation started in various sections of the reservoir. As a result of the CO_2-EOR, the field's oil production rate increased approximately 118 percent over the course of 13 years until 1998, when it started to decline again. This reservoir is one of the best examples to demonstrate clearly the effect of CO_2-EOR on a reservoir's oil production rate and cumulative production. The details of both waterflood and CO_2-EOR declines and the obtained relevant DCA equations and parameters are presented in figure C1–7.

Case Study 8. Clear Fork Group, Dollarhide Oil Field

The Clear Fork Group in the Dollarhide oil field in the Permian Basin in Texas is an oil-bearing carbonate (dolomite) formation that was under CO_2-EOR operations in 2012. On the basis of its OOIP, the Clear Fork Group in this field is classified as a medium-sized oil reservoir. The waterflood decline of the field started in 1970 and continued until 1977. On the basis of the available production data, it is not possible to investigate what happened between 1977 and 1995, during which time the reservoir oil production rate stopped declining and increased slightly. This change in the oil production decline could be due to infill drilling and (or) changes in the waterflood scheme in different sections of the reservoir. In November 1995, the CO_2-EOR operation started in this reservoir. As a result of the CO_2-EOR, the field's oil production rate increased approximately 139 percent over the course of 4 years until 1999, when it started to decline again. The details of both waterflood and CO_2-EOR declines and the obtained relevant DCA equations and parameters are presented in figure C1–8.

Case Study 9. "Canyon-age reservoir," Salt Creek Oil Field

The "Canyon-age reservoir" in the Salt Creek oil field in the Permian Basin in Texas is an oil-bearing carbonate (limestone) formation that was under CO_2-EOR operations in 2012. On the basis of its OOIP, the "Canyon-age reservoir" in this field is classified as a large oil reservoir. The waterflood decline of the field started in 1972 and continued until 1993, when the CO_2-EOR operation started in various sections of the reservoir. As a result of the CO_2-EOR, the field's oil production rate increased approximately 38 percent over the course of 4 years until 1997, when it started to decline again. The details of both waterflood and CO_2-EOR declines and the obtained relevant DCA equations and parameters are presented in figure C1–9.

Case Study 10. San Andres Limestone, Seminole Oil Field

The San Andres Limestone in the Seminole oil field in the Permian Basin in Texas is an oil-bearing carbonate (dolomite) formation that was under CO_2-EOR operations in 2012. On the basis of its OOIP, the San Andres Limestone in this field is classified as a large oil reservoir. The waterflood decline of the field started in 1977 and continued until 1983, when the CO_2-EOR operation started in various sections of the reservoir.

As a result of the CO_2-EOR, the field's oil production rate increased approximately 37 percent over the course of 8 years until 1991, when it started to decline again. The details of both waterflood and CO_2-EOR declines and the obtained relevant DCA equations and parameters are presented in figure C1–10.

Case Study 11. Ramsey Member, Twofreds Oil Field

The Ramsey Member of the Bell Canyon Formation in the Twofreds oil field in the Permian Basin in Texas contains an oil-bearing sandstone that was under CO_2-EOR operations in 2012. On the basis of its OOIP, the sandstone of the Ramsey Member in this field is classified as a small oil reservoir. The waterflood decline of the field started in 1967 and continued until 1974, when the CO_2-EOR operation started in various sections of the reservoir. As a result of the CO_2-EOR, the field's oil production rate increased approximately 323 percent over the course of 11 years until 1985, when it started to decline again. The details of both waterflood and CO_2-EOR declines and the obtained relevant DCA equations and parameters are presented in figure C1–11.

Case Study 12. San Andres Limestone, Vacuum Oil Field

The San Andres Limestone in the Vacuum oil field in the Permian Basin in New Mexico is an oil-bearing carbonate (dolomite) formation that was under CO_2-EOR operations in 2012. On the basis of its OOIP, the San Andres Limestone in this field is classified as a large oil reservoir. The waterflood decline of the field started in 1983 and continued until 1997, when the CO_2-EOR operation started in various sections of the reservoir. As a result of the CO_2-EOR, the field's oil production rate stayed stable until 2001, when it started to decline again. The details of both waterflood and CO_2-EOR declines and the obtained relevant DCA equations and parameters are presented in figure C1–12.

Case Study 13. San Andres Limestone, Cedar Lake Oil Field

The San Andres Limestone in the Cedar Lake oil field in the Permian Basin in Texas is an oil-bearing carbonate (dolomite) formation that was under CO_2-EOR operations in 2012. On the basis of its OOIP, the San Andres Limestone in this field is classified as a medium-sized oil reservoir. The waterflood decline of the field started in 1983 and continued until 1994, when the CO_2-EOR operation started in various sections of the reservoir. As a result of the CO_2-EOR, the field's oil production rate increased approximately 25 percent over the course of 7 years until 2001, when it started to decline again. The details of both waterflood and CO_2-EOR declines and the obtained relevant DCA equations and parameters are presented in figure C1–13.

Case Study 14. San Andres Limestone, North Hobbs Oil Field

The San Andres Limestone in the North Hobbs oil field in the Permian Basin in New Mexico is an oil-bearing carbonate (dolomite) formation that was under CO_2-EOR operations in 2012. On the basis of its OOIP, the San Andres Limestone in this field is classified as a small oil reservoir. The waterflood decline of the field started in 2000 and continued until 2003, when the CO_2-EOR operation started in various sections of the reservoir. As a result of the CO_2-EOR, the field's oil production rate increased approximately 104 percent over the course of 3 years until 2006, when it started to decline again. The details of both waterflood and CO_2-EOR declines and the obtained relevant DCA equations and parameters are presented in figure C1–14.

Case Study 15. San Andres Limestone, Yates Oil Field

The San Andres Limestone in the Yates oil field in the Permian Basin in Texas is an oil-bearing carbonate (dolomite) formation that was under CO_2-EOR operations in 2012. It should be noted that unlike the previous examples, the CO_2-EOR operation in this field is immiscible. On the basis of its OOIP, the San Andres Limestone in this field is classified as a large oil reservoir. The waterflood decline of the field started in 2000 and continued until 2004, when the CO_2-EOR operation started in various sections of the reservoir. As a result of the CO_2-EOR, the field's oil production rate increased approximately 48 percent over the course of 2 years until 2006, when it started to decline again. The details of both waterflood and CO_2-EOR declines and the obtained relevant DCA equations and parameters are presented in figure C1–15.

Reference Cited

IHS Inc., 2012, PIDM [Petroleum Information Data Model] relational U.S. well data [data current as of December 23, 2011]: Englewood, Colo., IHS Inc.

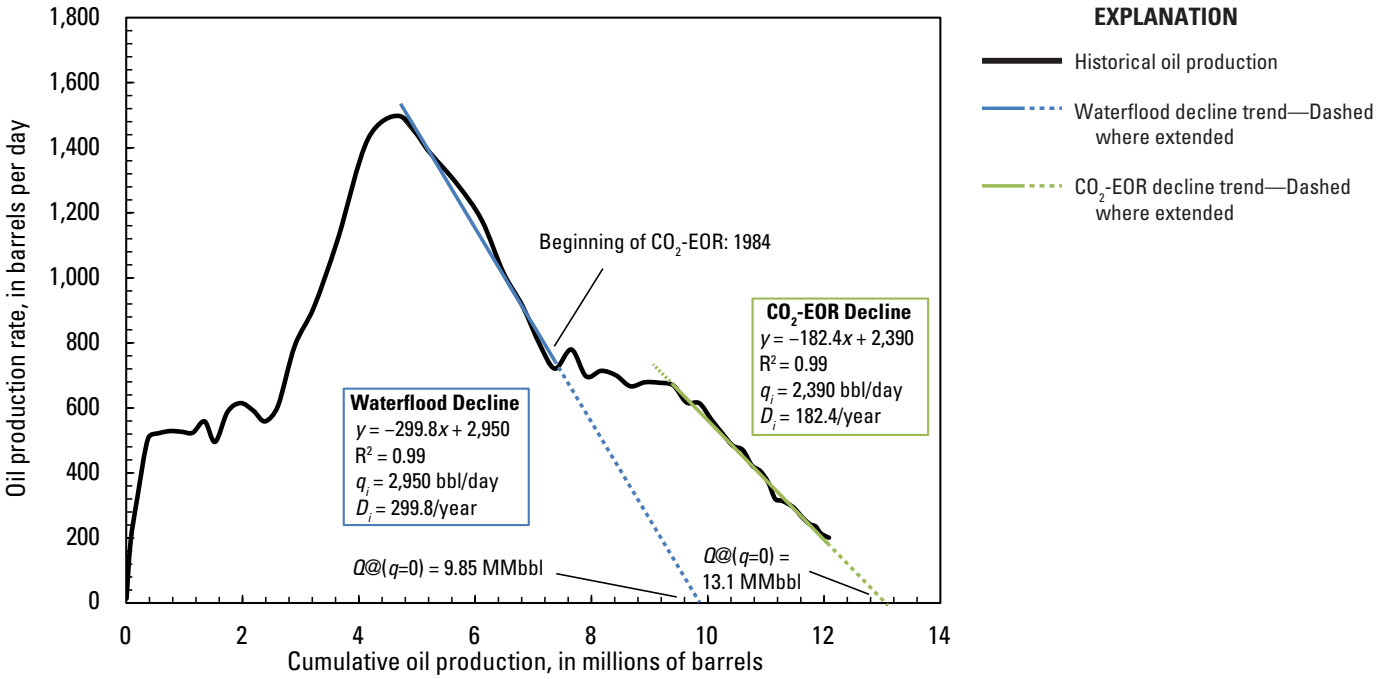

Figure C1–1. Graph of the oil production rate versus the cumulative oil production for the San Andres Limestone in the Sable oil field, Texas, showing the decline trends for both the waterflood and the carbon dioxide enhanced oil recovery (CO_2-EOR) phases. Data are from IHS Inc. (2012). Terms used in the decline equations on the graph: D_i = initial decline rate per year; q = oil production rate, in barrels per day (bbl/day); q_i = initial oil production rate, in barrels per day (bbl/day); Q = cumulative oil production, in millions of barrels (MMbbl); R^2 = coefficient of determination; x = cumulative oil production in the trendline equation, in millions of barrels; y = oil production rate in the trendline equation, in barrels per day.

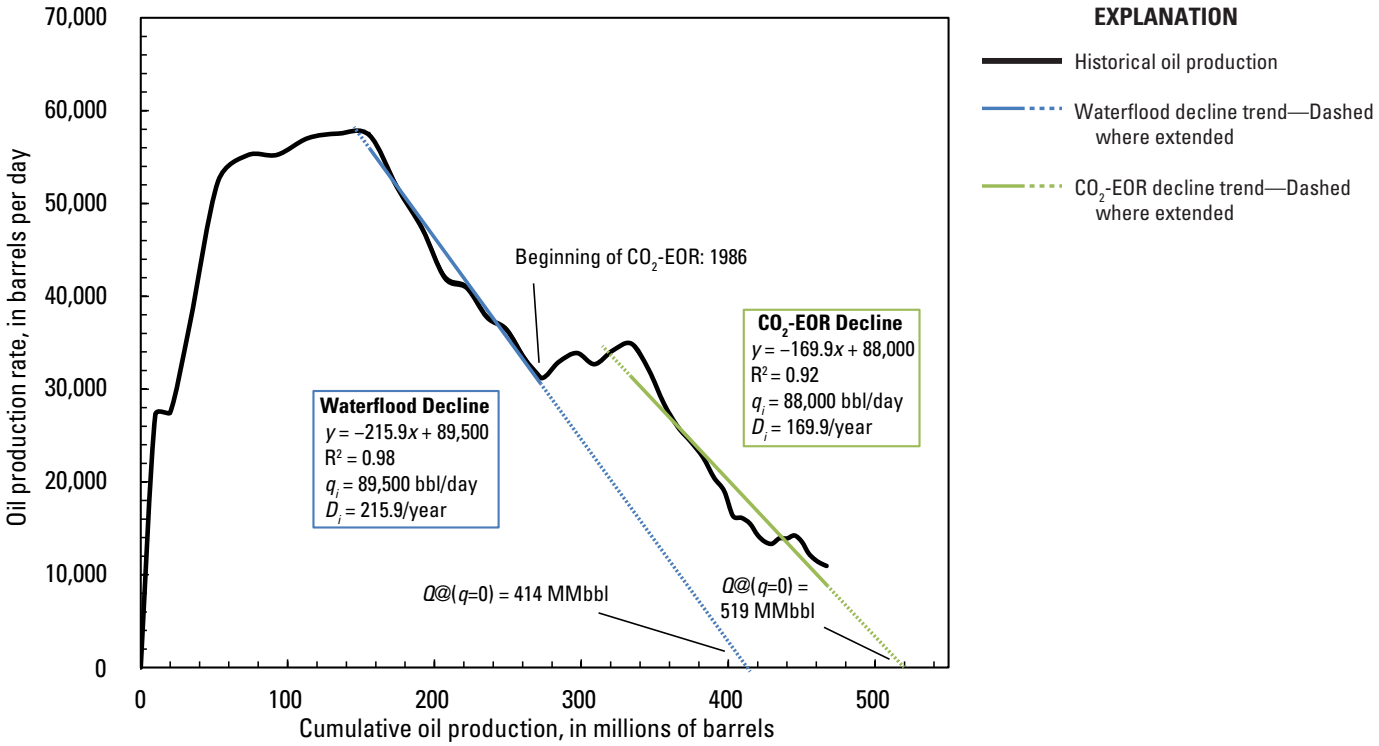

Figure C1–2. Graph of the oil production rate versus the cumulative oil production for the Weber Sandstone in the Rangely oil field, Colorado, showing the decline trends for both the waterflood and the carbon dioxide enhanced oil recovery (CO_2-EOR) phases. Data are from IHS Inc. (2012). Terms are as defined for figure C1–1. For completeness, this figure is included in the appendix even though it is also shown as text-figure C2.

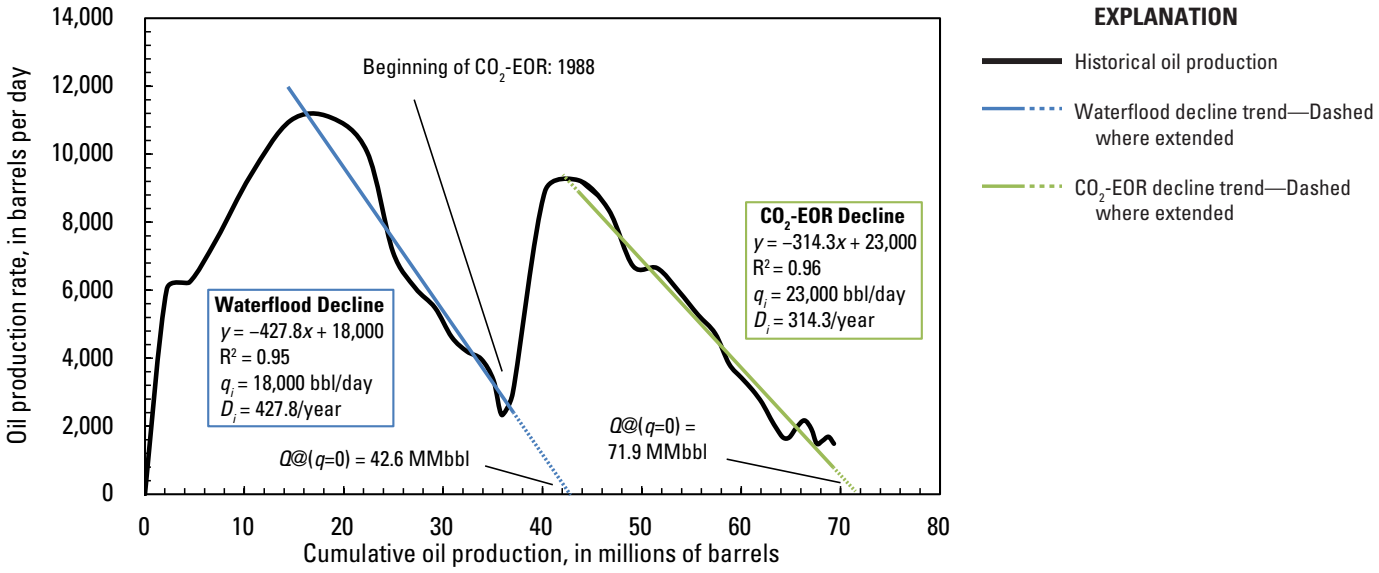

Figure C1–3. Graph of the oil production rate versus the cumulative oil production for the Tensleep Formation in the Lost Soldier oil field, Wyoming, showing the decline trends for both the waterflood and the carbon dioxide enhanced oil recovery (CO_2-EOR) phases. Data are from IHS Inc. (2012). Terms are as defined for figure C1–1.

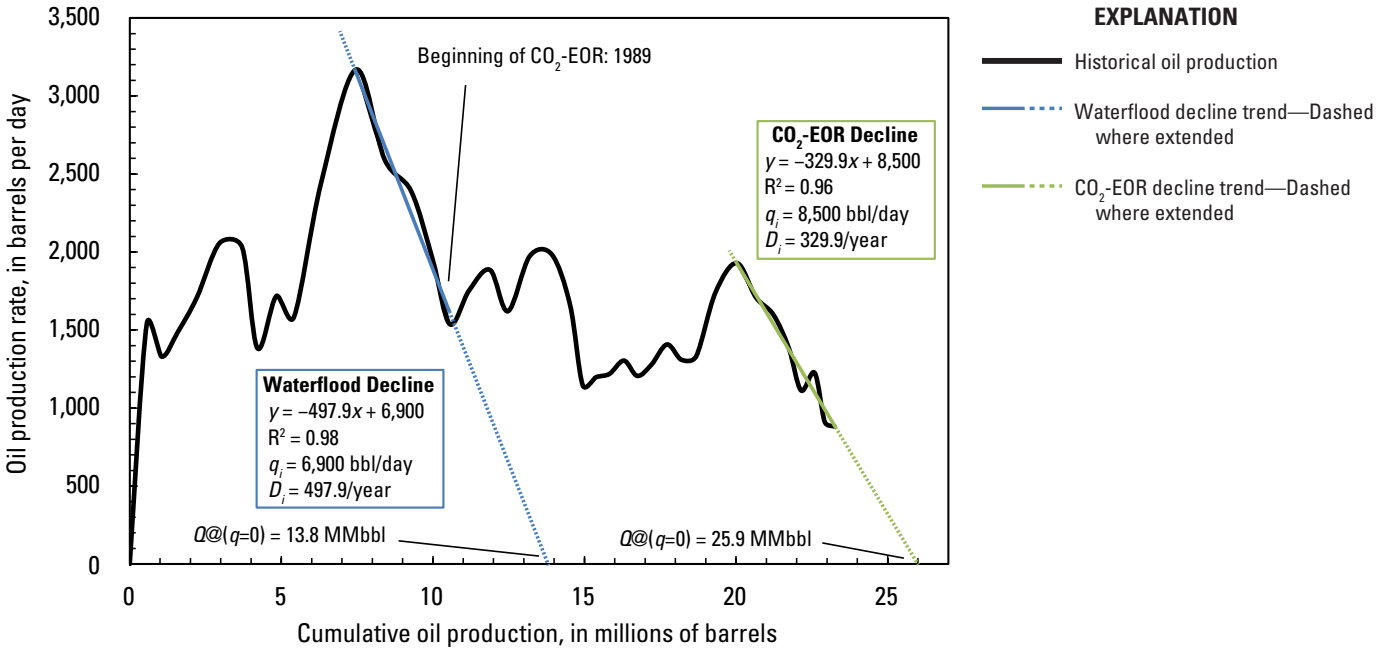

Figure C1–4. Graph of the oil production rate versus the cumulative oil production for the Madison Formation in the Lost Soldier oil field, Wyoming, showing the decline trends for both the waterflood and the carbon dioxide enhanced oil recovery (CO_2-EOR) phases. Data are from IHS Inc. (2012). Terms are as defined for figure C1–1.

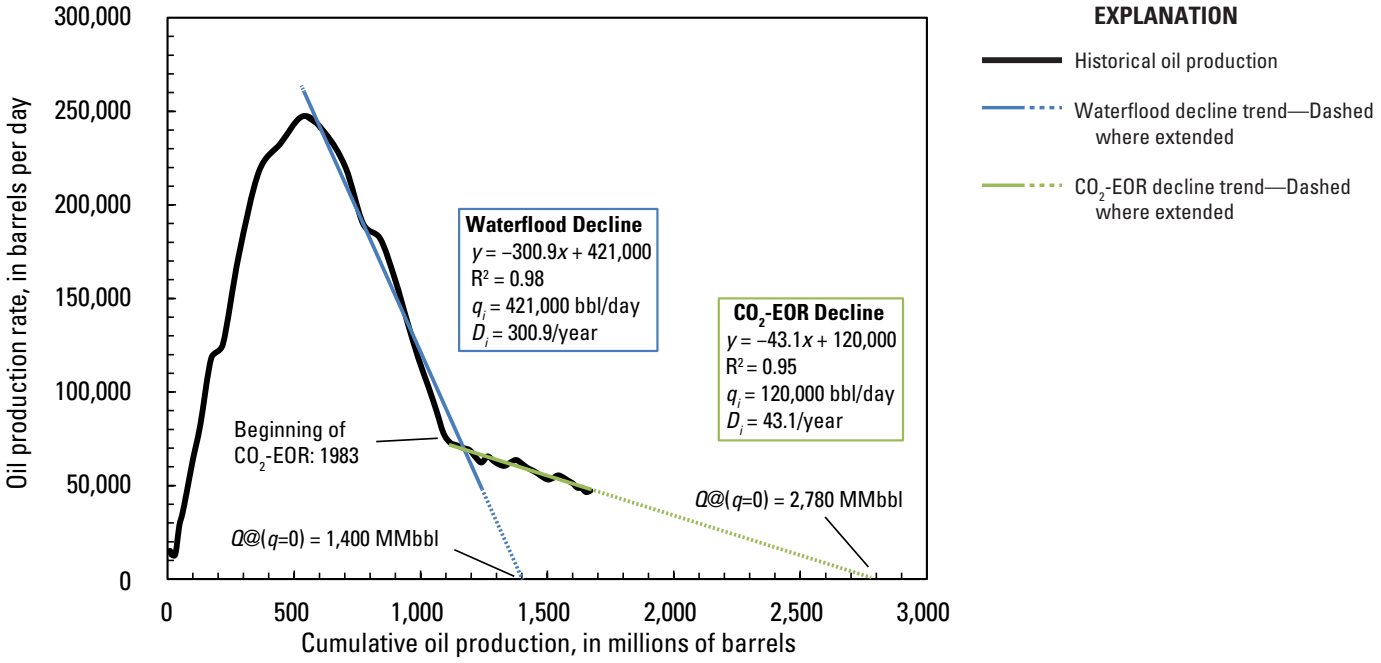

Figure C1–5. Graph of the oil production rate versus the cumulative oil production for the San Andres Limestone in the Wasson oil field, Texas, showing the decline trends for both the waterflood and the carbon dioxide enhanced oil recovery (CO_2-EOR) phases. Data are from IHS Inc. (2012). Terms are as defined for figure C1–1.

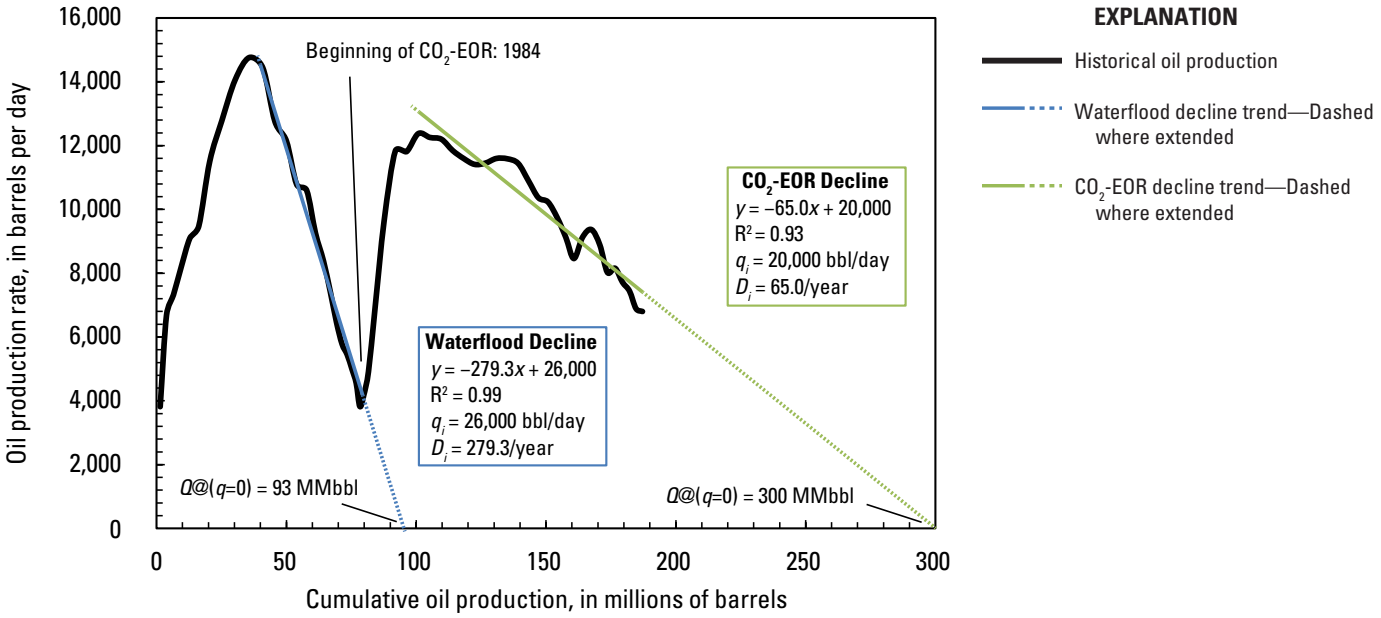

Figure C1–6. Graph of the oil production rate versus the cumulative oil production for the Clear Fork Group in the Wasson oil field, Texas, showing the decline trends for both the waterflood and the carbon dioxide enhanced oil recovery (CO_2-EOR) phases. Data are from IHS Inc. (2012). Terms are as defined for figure C1–1.

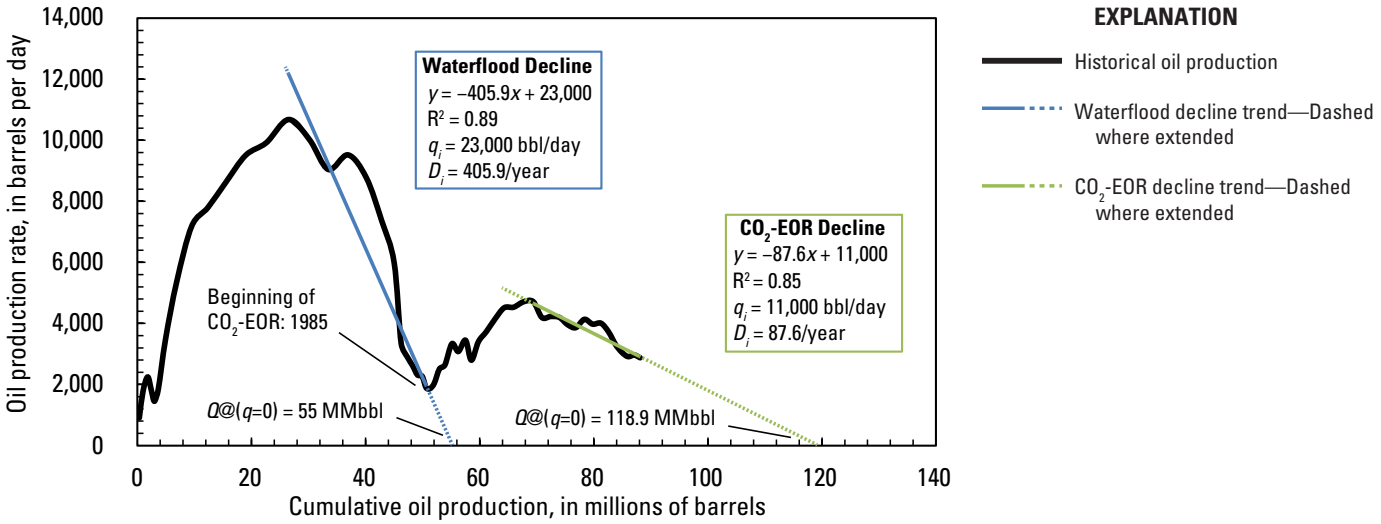

Figure C1–7. Graph of the oil production rate versus the cumulative oil production for the Thirtyone Formation in the Dollarhide oil field, Texas, showing the decline trends for both the waterflood and the carbon dioxide enhanced oil recovery (CO_2-EOR) phases. Data are from IHS Inc. (2012). Terms are as defined for figure C1–1.

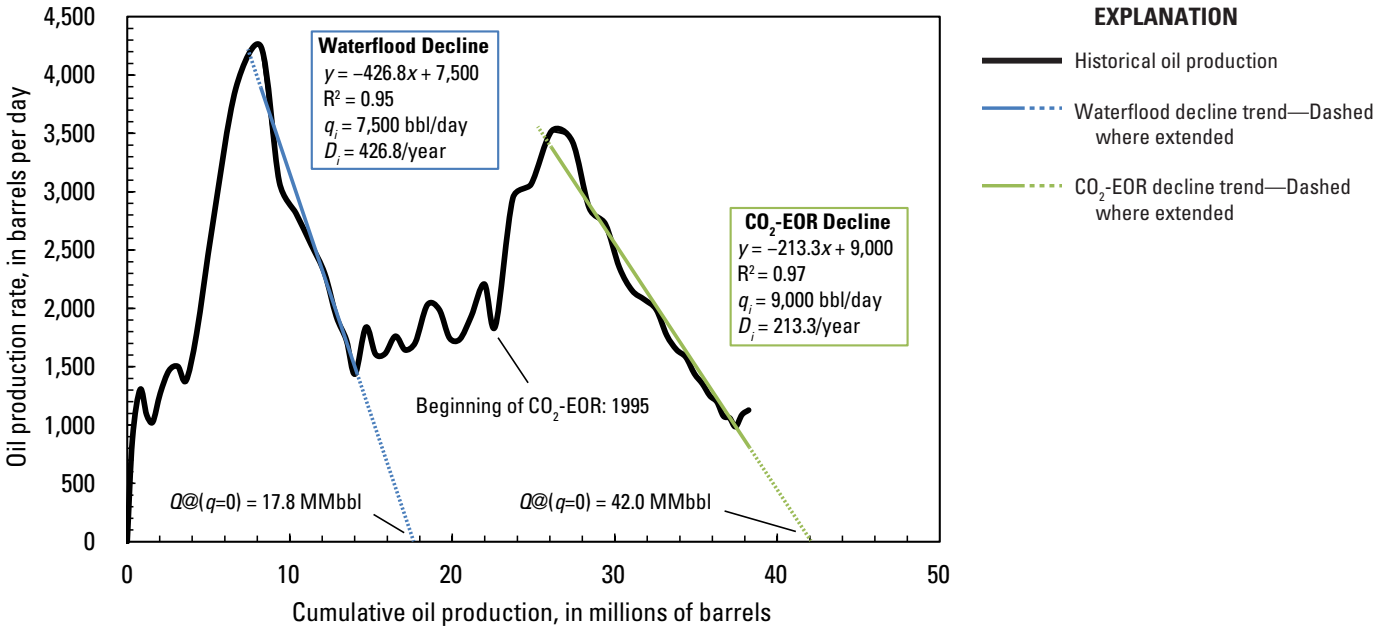

Figure C1–8. Graph of the oil production rate versus the cumulative oil production for the Clear Fork Group in the Dollarhide oil field, Texas, showing the decline trends for both the waterflood and the carbon dioxide enhanced oil recovery (CO_2-EOR) phases. Data are from IHS Inc. (2012). Terms are as defined for figure C1–1.

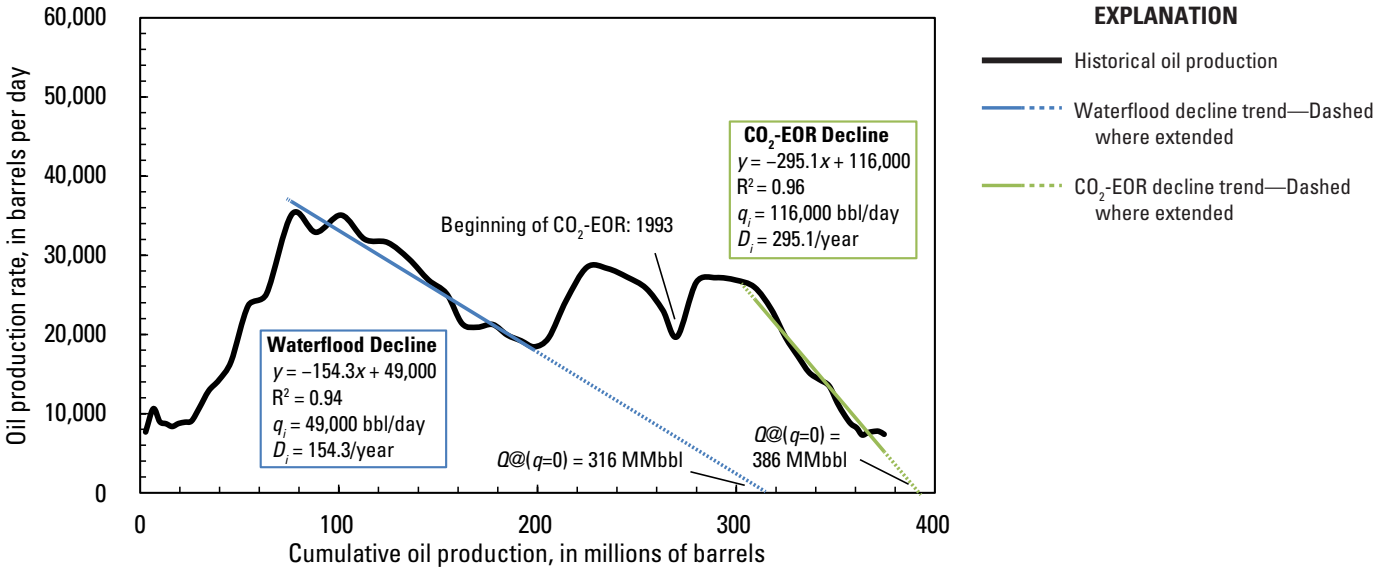

Figure C1–9. Graph of the oil production rate versus the cumulative oil production for the "Canyon-age reservoir" in the Salt Creek oil field, Texas, showing the decline trends for both the waterflood and the carbon dioxide enhanced oil recovery (CO_2-EOR) phases. Data are from IHS Inc. (2012). Terms are as defined for figure C1–1.

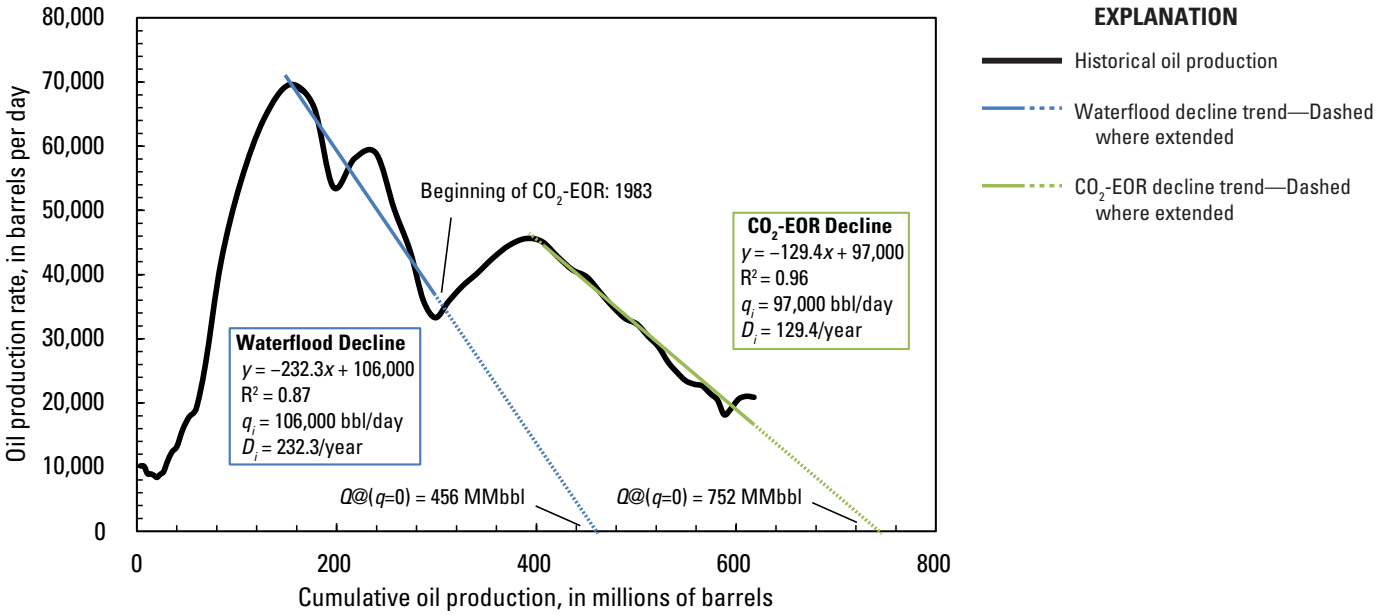

Figure C1–10. Graph of the oil production rate versus the cumulative oil production for the San Andres Limestone in the Seminole oil field, Texas, showing the decline trends for both the waterflood and the carbon dioxide enhanced oil recovery (CO_2-EOR) phases. Data are from IHS Inc. (2012). Terms are as defined for figure C1–1.

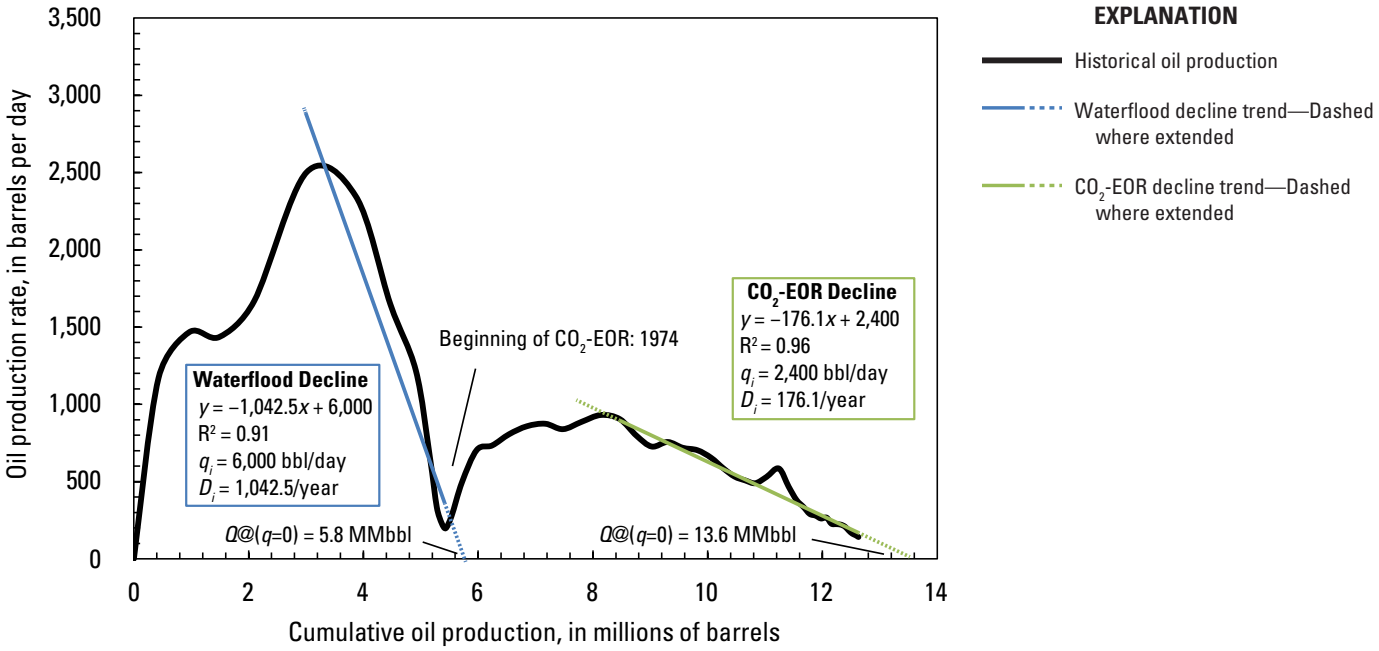

Figure C1–11. Graph of the oil production rate versus the cumulative oil production for the sandstone of the Ramsey Member of the Bell Canyon Formation in the Twofreds oil field, Texas, showing the decline trends for both the waterflood and the carbon dioxide enhanced oil recovery (CO_2-EOR) phases. Data are from IHS Inc. (2012). Terms are as defined for figure C1–1.

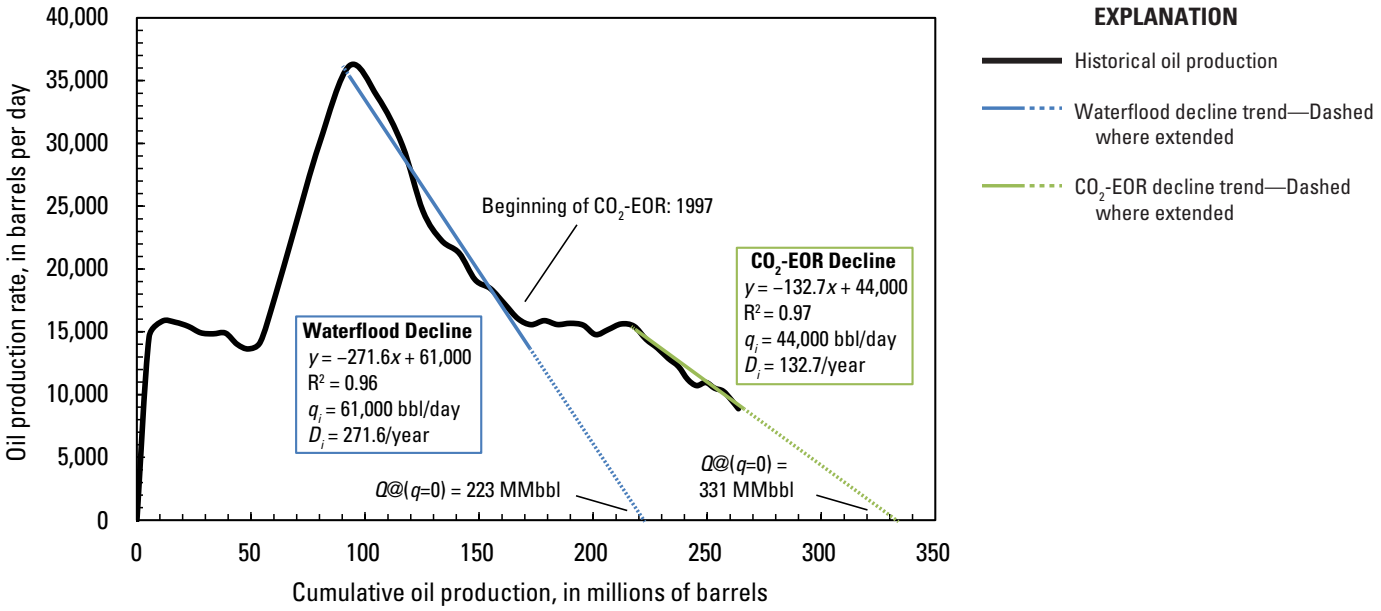

Figure C1–12. Graph of the oil production rate versus the cumulative oil production for the San Andres Limestone in the Vacuum oil field, New Mexico, showing the decline trends for both the waterflood and the carbon dioxide enhanced oil recovery (CO_2-EOR) phases. Data are from IHS Inc. (2012). Terms are as defined for figure C1–1.

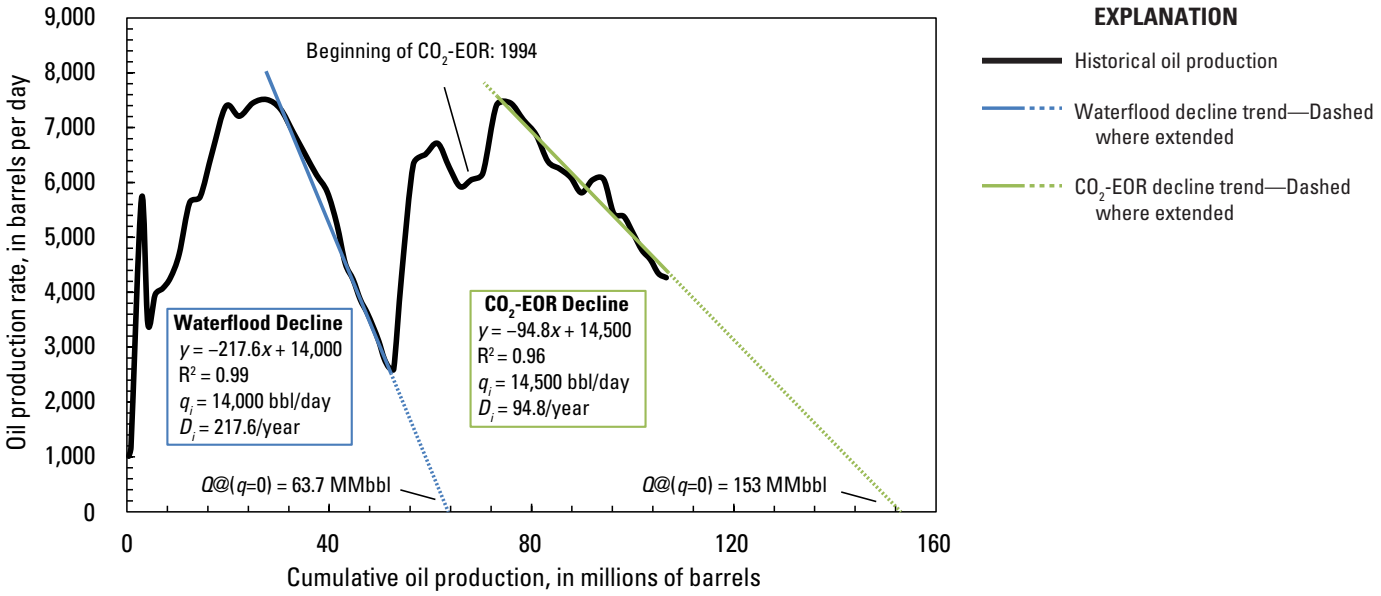

Figure C1–13. Graph of the oil production rate versus the cumulative oil production for the San Andres Limestone in the Cedar Lake oil field, Texas, showing the decline trends for both the waterflood and the carbon dioxide enhanced oil recovery (CO_2-EOR) phases. Data are from IHS Inc. (2012). Terms are as defined for figure C1–1.

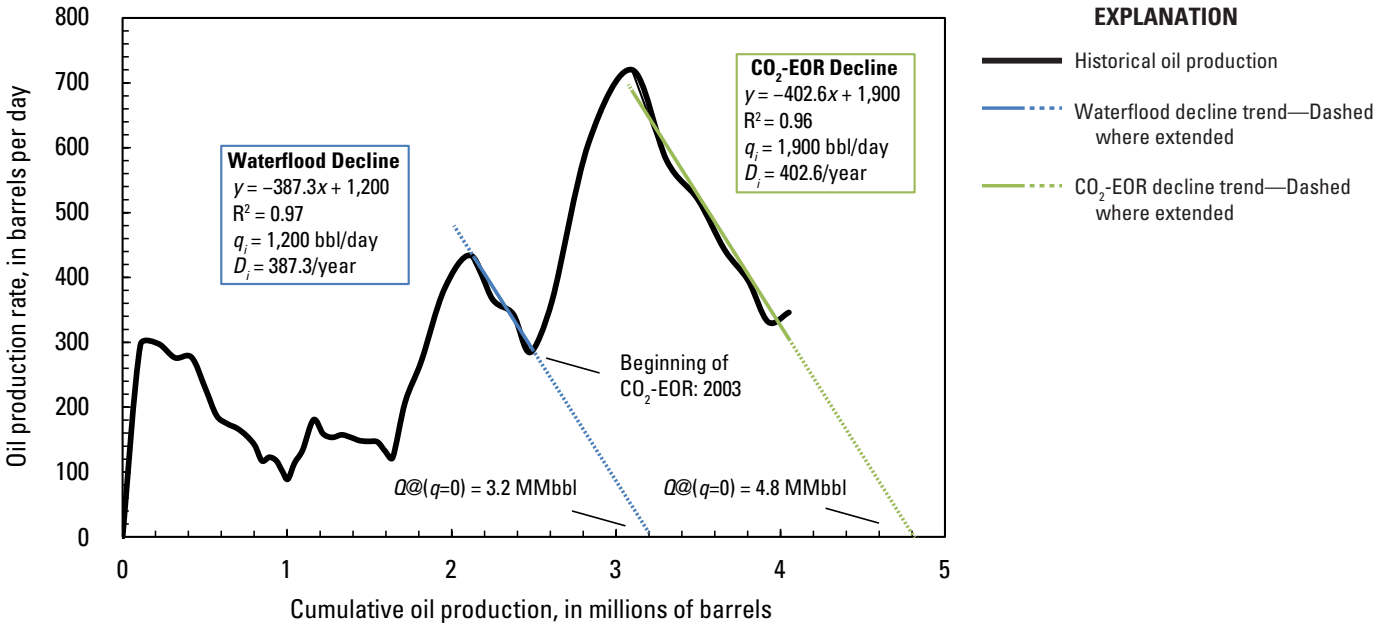

Figure C1–14. Graph of the oil production rate versus the cumulative oil production for the San Andres Limestone in the North Hobbs oil field, New Mexico, showing the decline trends for both the waterflood and the carbon dioxide enhanced oil recovery (CO_2-EOR) phases. Data are from IHS Inc. (2012). Terms are as defined for figure C1–1.

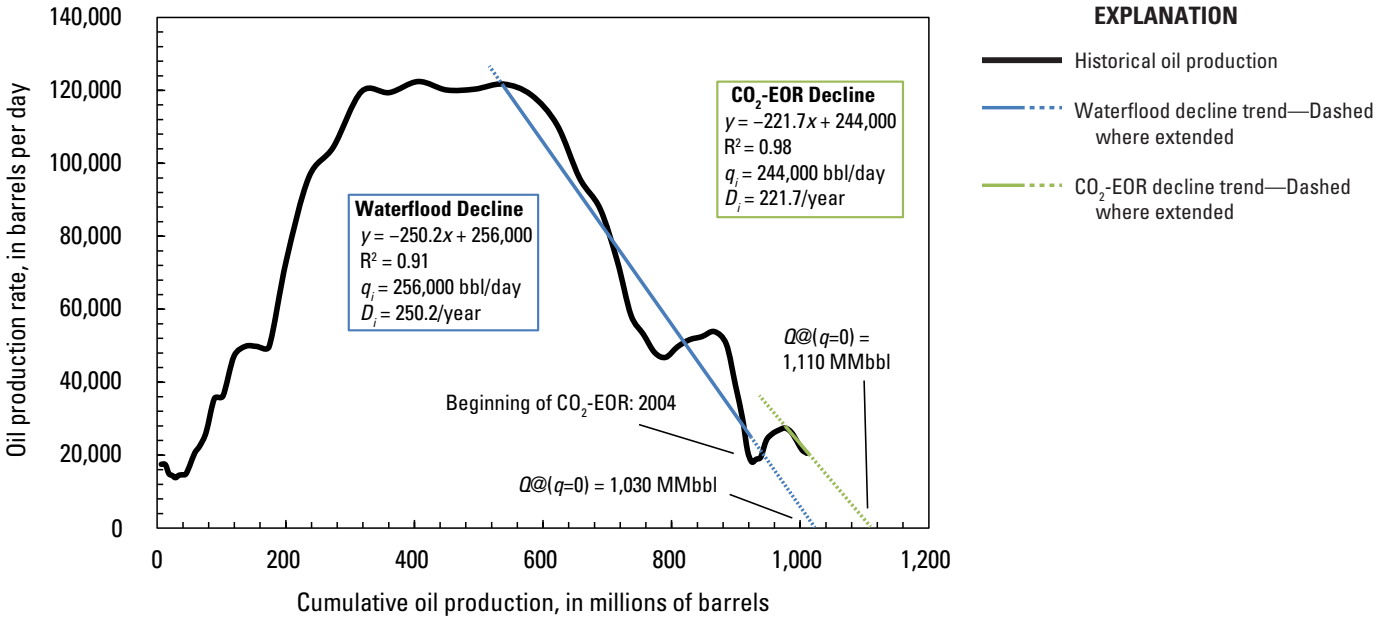

Figure C1–15. Graph of the oil production rate versus the cumulative oil production for the San Andres Limestone in the Yates oil field, Texas, showing the decline trends for both the waterflood and the carbon dioxide enhanced oil recovery (CO_2-EOR) phases. Data are from IHS Inc. (2012). Terms are as defined for figure C1–1.